Available online at www.sciencedirect.com
ScienceDirect
Journal of Photochemistry and Photobiology A: Chemistry 183 (2006) 35–40
Journal of Photochemistry and Photobiology A:Chemistry
www.elsevier.com/locate/jphotochem

Photocatalytic oxidation of aldehydes: Byproduct identification and reaction pathway

Xuejun Ye, Daniel Chen *, John Gossage, Kuyen Li

Department of Chemical Engineering, Lamar University, Beaumont, TX 77710, United States

Received 19 September 2005; received in revised form 28 December 2005; accepted 13 February 2006
Available online 6 March 2006

Abstract

The byproducts and reaction pathway of gas phase photocatalytic oxidation (PCO) of butyraldehyde, propionaldehyde and acetaldehyde over aerogel TiO_2 under weak black light were studied by means of liquid nitrogen trapping, water extraction, mass spectrometry and carbon balance. Aldehydes were photocatalytically oxidized to corresponding acids, shorter carbon-chain aldehydes, carbon dioxide and water. The so-generated acids were further oxidized to shorter carbon-chain aldehydes, carbon dioxide, and water. Other side reactions were suppressed. The reaction pathway we found can be explained in a straightforward manner with active O^* as well as hydroxyl group as the major oxidants.

Keywords: Photocatalysis; Aldehyde; Byproduct identification; Titania; Reaction pathway; Mechanism

1. Introduction

Photocatalysis emerged as a promising technology in 1972 when Fujishima and Honda split water into oxygen and hydrogen with a TiO_2–Pt element [1]. In addition to water splitting for fuel cell applications, photocatalysis is attractive in air and water pollution control due to its potential to use solar energy. For photocatalytic oxidation (PCO), illumination of UV or visible light on semiconductors, such as TiO_2, generates highly reactive electron–hole pairs that can oxidize volatile organic compounds (VOC's) or nitrogen oxides (NO_x) at ambient conditions. Since sunlight has about 4% UV and up to 40% visible light, using the visible spectrum to increase the efficiency of PCO [2] is of great interest. In fact, practical applications of PCO using sunlight and room lighting are being developed world-wide. For example, Westminster Borough of London cooperated with Japan's Mitsubishi Materials Corporation to pave roads with TiO_2 containing paving stone [3]. Under an intensity of UV light of 1–12 watts per square meter (W/m^2), an 80% NO_x removal rate was achieved in the test. The Central Research Institute of Electric Power Industry in Japan has developed a titanium oxide photocatalyst film with deodorant, antibacterial, antifogging, and self-cleaning effects for room use under weak-ultraviolet rays. Tests showed that 25% of actaldehyde was decomposed in 30 h [4].

Complete mineralization of pollutants is usually not done for PCO using sunlight and room lighting unless a very long residence time is allowed. Therefore, byproducts and reaction pathways should be identified for safety and health reasons. Especially, some byproducts may be more hazardous than the parent compound. The federal Emergency Planning and Community Right-to-know Act (EPCRA) of 1986 established the List of Toxic Chemicals, also referred to as the toxics release inventory (TRI). Butyraldehyde, propionaldehyde, acetaldehyde, and formaldehyde are all TRI toxics, as they may cause significant adverse acute effects on health or damage to the environment [5]. These aldehydes all are high volume chemicals (>1 million pounds/year) used in consumer products that contribute to indoor air pollution [6]. In 1992, the U.S. production volume of butyraldehyde was 1.8 billion pounds [7], while U.S. production of acetaldehyde was estimated to be 740 million pounds in 1989 [8].

At present, the understanding is very limited regarding byproducts and pathways of aldehyde PCO. Huang et al. [9] used an active carbon column to adsorb products of butyraldehyde PCO, and then heated the carbon column from 50 to 320 °C to release the adsorbates. Eight major compounds (butyraldehyde, acetaldehyde, propionaldehyde, ethanol, 1-propanol, formic

* Corresponding author. Tel.: +1 409 8808786; fax: +1 409 8802197.
E-mail address: chendh@hal.lamar.edu (D. Chen).

1010-6030/$ – see front matter © 2006 Elsevier B.V. All rights reserved.
doi:10.1016/j.jphotochem.2006.02.019

acid propyl ester, di-*n*-propyl-ether, and 3-heptene) and 14 minor compounds were detected in the desorption flow. Since active carbon possesses considerable catalytic properties and can catalyze a number of oxidation, hydrolytic and decomposition reactions [10] during a thermo-desorption process, thermo-catalysis may happen and cause original byproducts of aldehyde PCO to disappear and new compounds to form. Huang et al. [9] also noticed the potential problems of using active carbon to collect byproducts, and considered that compounds detected at low temperatures are most likely the byproducts of butyraldehyde PCO.

Other researchers found much fewer outlet compounds in similar studies like butanol PCO, etc. Chapuis et al. [11] found that butyraldehyde and propionaldehyde were major byproducts of butanol PCO, while the third of detected byproducts was not identified. Peral and Ollis [12] observed two byproduct peaks in butanol PCO: one was identified as butyraldehyde with a retention time match, and the other was not identified. Under strong UV irradiation, Benoit-Marquie et al. [13] studied PCO of butanol with concentrations from 900 to 5000 mg/m^3 and observed six major byproducts (butyraldehyde, butyric acid, 1-propanol, propionaldehyde, ethanol and acetaldehyde). A challenge in identifying byproducts is that their low concentrations are often below instrument detection limits, and their concentrations cannot be effectively increased with higher reactant concentrations. A higher inlet concentration usually results in a lower conversion at a given reaction time, as with the assumption of plug flow photocatalysis rates have been well expressed with the Langmuir–Hinshelwood rate forms both in the literature [14,15] and our observations on aldehyde PCO.

In this study we use liquid nitrogen to condense, trap and concentrate gaseous byproducts from the effluent, then evaporate the condensed phase for identification with mass spectrometry. This technique is capable of enhancing the chances to identify byproducts, as the byproducts are effectively concentrated. Non-volatile organic compounds may not be collected with this design, but they do not likely exist in aldehyde PCO and usually do not cause direct air pollution. Side reactions of byproducts are minimized, since the sampling operates at very low temperatures. All detected compounds come directly from PCO. Extracted with deionized water, byproducts on the photocatalyst are also identified. The byproducts identified enable us to have a clear picture of the aldehyde PCO pathways. They can be explained in a straightforward manner with active O^* as well as hydroxyl group as the major oxidants.

2. Experimental

Aldehyde PCO's were conducted in a quartz tubular reactor (Ø 55 mm × 120 mm). Two hundred seventy-five pieces of optical fibers (Ø 0.2 mm × 120 mm) are evenly dispersed in the reactor along the axial direction so that UV irradiation can be well received. The reactor is wrapped with aluminum foil to decrease light loss. Coated on the surface of the optical fibers is 1.4 mg/cm^2 of LUAG2, a nano-size TiO_2 powder synthesized with the aerogel method. LUAG2 has the anatase form, a surface area of 237 m^2/g and a porosity of 0.31 [15]. In the center of the reactor, a 4 W UVA lamp (FL4BL, NEC), Ø 16 mm × 150 mm, is placed axially. Fibers are used as the support to improve the efficiency of the UV light transmission to the coated catalyst. The UV output of the lamp is 0.3 W while the photocatalyst coating area is 207 cm^2. The ratio of UV output to the coating area is 1.45 mW/cm^2.

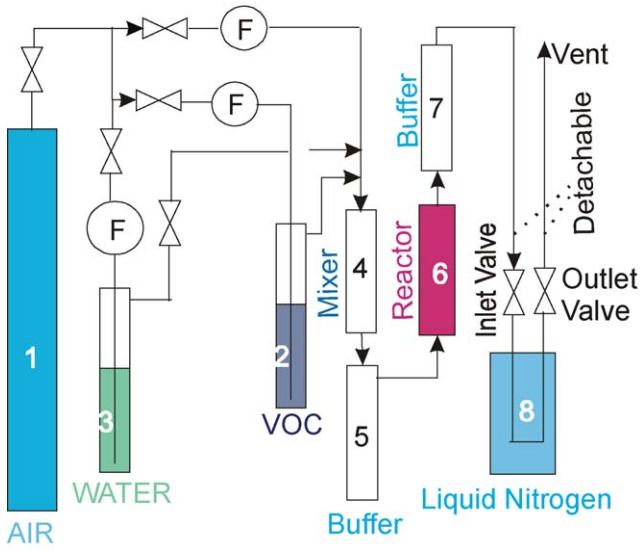

Fig. 1. Flowchart of the experimental apparatus.

As shown in Fig. 1, instrument air (# 1, Aeriform) is branched into three flows. One bubbles through gas wash bottle (# 2) filled with aldehydes, another passes through water (# 3) to obtain desired humidity, and the third goes directly through the in-line static pipe mixer (# 4, Cole-Parmer). All flows can be regulated independently to adjust the aldehyde concentration, humidity and total flowrate. The chosen mixer can dilute saturated VOC vapor to tens ppm. The mixed gas passes through an empty bottle (# 5) before entering the reactor (# 6). The buffer (# 5) can minimize the inlet concentration fluctuation resulting from vacuum sampling. Not shown are two pieces of sampling tubing before and after the reactor. They connect to a gas chromatography (GC) to monitor inlet and outlet aldehyde concentrations. The GC is a Varian Star 3400 with a flame-ionization detector (FID), and a 0.53 mm × 30 m bentone 34 di-*n*-decylphthalate column, operating at 210 °C injector, 190 °C oven and 220 °C detector. CO_2 concentrations are measured at the system outlet with a portable CO_2 analyzer (GD444, CEA Instruments, Inc.).

The effluent gas from the reactor then passes through a buffer (# 7) and then a cryogenic device (# 8, Fig. 1) to collect and concentrate gaseous byproducts. The device, made of 1/8″ stainless steel tubing coil, tees, stopper and valves, is airtight. The coil, around 1 m long and immersed in a 10 L liquid nitrogen (−195.4 °C at 101.3 kPa) tank, is able to condense or freeze alcohols and aldehydes [16]. The byproducts are accumulated in the coil until it can supply at least six analyses. The accumulation of byproducts usually takes 2–12 h depending on their concentrations and vapor pressure. Then valves on either end of the collection device are closed and the device is removed from the liquid nitrogen tank. As its temperature

rises to room temperature, condensed byproducts will vaporize. The final pressure can be 400 kPa after the temperature reaches room temperature. Then the device is connected to a GC/mass spectrometry (MS) sampling line for byproduct identification of the concentrated gas sample.

The GC/MS is a quadrupole HP GCD1800B, with a HP-5 (crosslinked 5% PH ME siloxane) 30 m × 0.25 mm × 0.25 μm column, electron ionization detector (EID) with mass range of 10–425 *m/z* (mass to charge ratio) and HP ChemStation software. Its detection limit is estimated to be 5 ppm. The mass spectral libraries installed are Wiley275 (275,000 spectra) and NBS75k (75,000 spectra). The GC/MS has an on-line vacuum sampling mechanism to take 250 μL sample each time so that good repeatability is obtained. The prepared gas sample above mentioned is enough to be analyzed at least six times. The chromatographic parameters for gas sample are 30 °C for column, 130 °C for injection port, 60 °C for detector, 0.7 ml/min for helium flow, splitless injection, and 35:200 *m/z* for mass range.

Byproducts adsorbed on the bulk of the catalyst are also detected. The reaction time must be long enough so that the byproduct concentrations in the later prepared liquid samples are much higher than the GC/MS detection limit. It is also determined by trial and error and usually takes at least 6 h. Then, the 275 pieces of optical fibers coated with photocatalyst are removed out of the reactor and immersed in 3 mL of deionized water in a measuring cylinder inside an ultrasonic cleaner (Model FS 60, Fisher Scientific). After 20 min ultrasonic operation, TiO_2 particles fully drop off from the optical fibers, and disperse in water. We use only deionized water to extract components from optical fibers, because we expected that the aldehyde PCO byproducts to be polar in the presence of oxygen. The expectation referred the byproducts mentioned in literature [9,11–13], and further confirmed by all the major byproducts identified in the gas and water phases in our observation. The formed suspension is then put into a 15 mL centrifuge tube. After spinning at 2100 rpm for 10 min in a centrifuge (Junior Angle #1600, Hamilton Bell Co. Inc.), TiO_2 is deposited on the bottom, and the clear top liquid is ready for GC/MS analysis. For a liquid sample, the GC/MS parameters are 50 °C oven, 130 °C inlet injection, 60 °C detector, 0.7 mL/min helium carrier gas flow rate, split injection, and 35:200 *m/z* of mass range.

3. Results and discussions

The kinetics of aldehyde PCO's was reported previously [15]. In the current study we focus on the byproduct identification and reaction pathway.

3.1. Byproducts from butyraldehyde PCO

In butyraldehyde PCO, butyraldehyde inlet concentrations vary from 30 to 243 ppm molar, and space–time range from 1 to 48 s with conversions from 50% to 90%. The space–time is defined as the reactor volume divided by the flowrate, and the conversion is one minus the ratio of the outlet concentration to the inlet concentration. It is confirmed that propionaldehyde and acetaldehyde are major byproducts in the gas phase. An

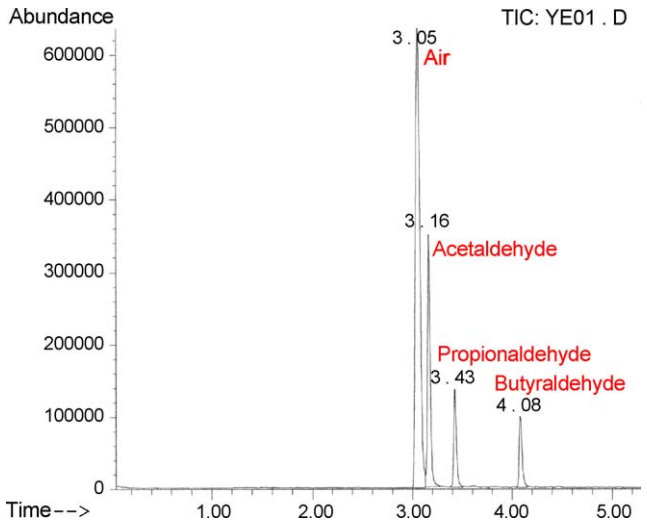

Fig. 2. GC spectrum at 90% conversion for the PCO of butyraldehyde.

output from the GC/MS is shown in Fig. 2. The blank tests with instrument air (Aeriform) and room air (400 ppm molar of CO_2) confirmed that the first peak (3.05 min) was the mixture of air and CO_2. Other peaks were butyraldehyde (4.08 min), propionaldehyde (3.43 min) and acetaldehyde (3.16 min) with convincing match qualities compared with the standard mass spectra in the mass spectral libraries. Their fragmentation patterns of the mass spectra were also checked with the standards. Also their retention times matched with those of commercial (Sigma–Aldrich) butyraldehyde (99.5%), propionaldehyde (97.0%) and acetaldehyde (99.0%). No additional compounds were observed from the gaseous effluent, even if within a much wider humidity range (3 ppm to 1.6 mol%) and space–time range (1–48 s).

To make sure all gas byproducts were collected and then evaporated, we let the reactor effluent pass through the cryogenic device for 24 h, and then heated the device to different temperatures ranging from 25 to 80 °C to vaporize organic products. While air plus CO_2, butyraldehyde, acetaldehyde and propionaldehyde peaks were detected, ethanol, 1-propanol, formic acid propyl ester, di-*n*-propyl-ether, and 3-heptene were not observed. Even though the vapor pressures of ethanol, 1-propanol, formic acid propyl ester, di-*n*-propyl-ether, and 3-heptene are lower than those of acetaldehyde and propionaldehyde, these compounds are volatile enough to be present in the vapor phase in the exit if produced. Therefore, those compounds detected by Huang et al. were likely generated through side reactions during the heating procedure in the activated carbon bed, as the authors [9] postulated.

Liquid samples obtained by washing the catalyst with deionized water were identified with the GC/MS system. A 0.15 μl sample was injected to the system manually. No peaks other than water were shown in the blank test of deionized water. A GC spectrum (Fig. 3) from liquid sampling showed four peaks: butyric acid (5.12 min), propionic acid (3.08 min), acetic acid (2.18 min) and water (1.60 min). Their retention times matched with those of commercial (Sigma–Aldrich) butyric (99.0%), propionic (≥99.5%) and acetic acid (≥99.7%). Note that the abundance in Fig. 3 is an order of magnitude smaller than that

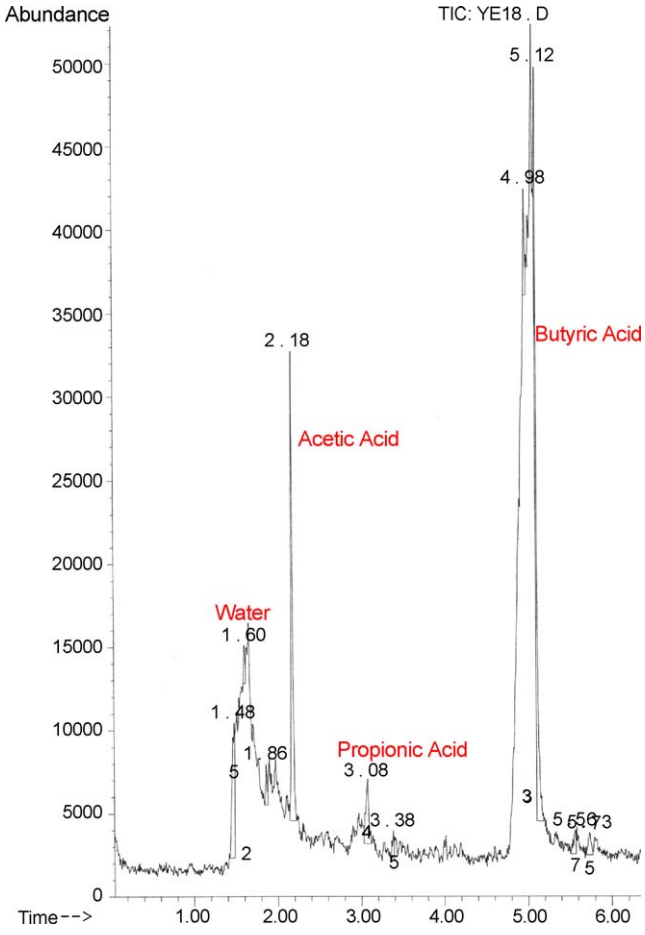

Fig. 3. GC spectrum of liquid sample of butyraldehyde PCO.

in Fig. 2, which makes the base line noise appear to be higher in Fig. 3 than in Fig. 2.

The acids all have a low vapor pressure and a high affinity to the photocatalyst and tubing, so that they might not show up in the gas phase detection. To confirm this, we conducted butyric acid PCO and found the strong adsorption of butyric acid in the stainless tubing and the TiO_2 catalyst, which resulted in its absence in the gas phase detection. Similarly, Blake and Griffin [17] also observed that butyric acid was not detected in the gas phase during butanol PCO over TiO_2, and the IR studies showed it was disappearing slowly on the photocatalyst surface.

3.2. Byproducts from propionaldehyde and acetaldehyde PCO

Propionaldehyde and acetaldehyde PCO's were done in the same manner described above. During propionaldehyde PCO, CO_2 and acetaldehyde were detected in the gas phase, and acetic and propionic acid were identified to be on the bulk of TiO_2 by means of water washing mentioned above [16]. Similarly, detected reaction products from acetaldehyde PCO were CO_2 in the gas phase, and formic acid and acetic acid on the photocatalyst [17]. The retention time of formic acid was checked with that of commercial formic acid (98–100%, Sigma–Aldrich). Of course water was a product of all PCO's mentioned above.

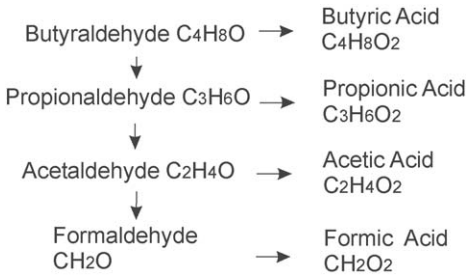

Fig. 4. The reaction pathway established experimentally from aldehyde PCO.

3.3. Reaction pathways of aldehyde PCO

Based on the compounds detected in the gas phase and on the photocatalyst, we experimentally established the reaction steps (Fig. 4.), except that we added acetaldehyde → formaldehyde, and formaldehyde → formic acid steps. Formaldehyde could not be detected because of its reactivity. Formic acid was not observed during butyraldehyde and propionaldehyde PCO. But we did detect formic acid during acetaldehyde PCO. The last two reaction steps were confirmed by the work of Muggli et al. [18], who used isotope labeling, temperature-programmed desorption (TPD) and oxidation (TPO) to study the reaction pathways and byproducts of ethanol PCO on Degussa P-25 TiO_2. In addition, Muggli et al. proposed that formaldehyde had to go through formic acid to become CO_2, as there was a time delay before the maximum desorption of CO_2 during formaldehyde PCO.

Based on the information above, we are confident that aldehyde PCO's generate corresponding acids, shorter carbon-chain aldehydes, CO_2 and water. We also ran butyric acid PCO under UVA light illumination to determine the fate of acids. We found propionaldehyde and acetaldehyde in the gas phase, and propionic and acetic acid on the photocatalyst. So the acids in PCO became shorter carbon-chain aldehydes, which were oxidized to the corresponding acids. It was not possible for acids to be directly oxidized to a shorter carbon-chain acid without going through a shorter carbon-chain aldehyde. Consequently we proposed reaction pathways as shown in Fig. 5.

This raises the following question: can shorter carbon-chain aldehydes come directly from longer carbon-chain aldehydes without going through acids first? For instance, can butyraldehyde become propionaldehyde directly without being oxidized to butyric acid first? In studying ethanol PCO, Muggli et al.

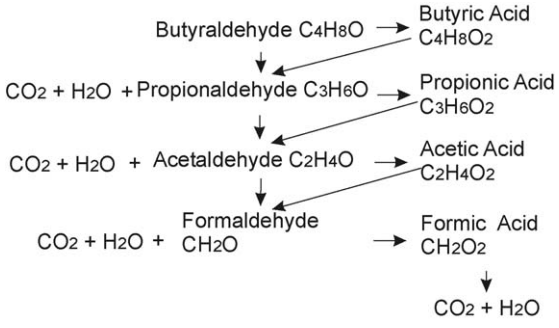

Fig. 5. Reaction pathways of butyraldehyde PCO.

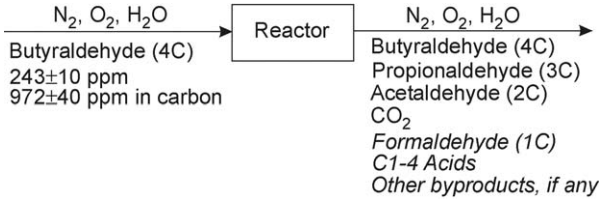

Fig. 6. Carbon balance.

[18] found that acetaldehyde could become formic acid and formaldehyde without going through acetic acid. Therefore, butyraldehyde PCO to propionaldehyde should have two pathways. One goes through butyric acid, and the other goes directly to propionaldehyde. CO_2 and water were, of course, products during each carbon scission. Fig. 5 summarized the reaction pathways discussed above.

3.4. Carbon balance of butyraldehyde PCO

The reaction pathway above was further checked with a carbon balance (Fig. 6). The outlet concentrations of propionaldehyde and acetaldehyde were measured with GC/FID. The CO_2 concentrations were measured with a CO_2 analyzer. The measurement of each concentration was repeated at least four times with a relative error of 4%. Formaldehyde, and formic, acetic, propionic and butyric acids could not be measured with GC/FID as mentioned before. At steady state, the total outlet carbon equals the total inlet carbon. The total carbon concentrations of unmeasured chemicals are calculated by the total outlet carbon concentration minus the total outlet carbon concentration of measured chemicals. Their maximum absolute error is 6.0% of the total inlet carbon.

As can be seen in Fig. 7, mineralization to CO_2 ranges from 10% to 85% depending on the space–time. The unmeasured chemicals (formaldehyde, C1-4 acids, and other byproducts, if any) account for from 18% to 45%. As formaldehyde and C1-4 acids should constitute important parts of the unmeasured chemicals, other byproducts, if any, should be in very small quantities.

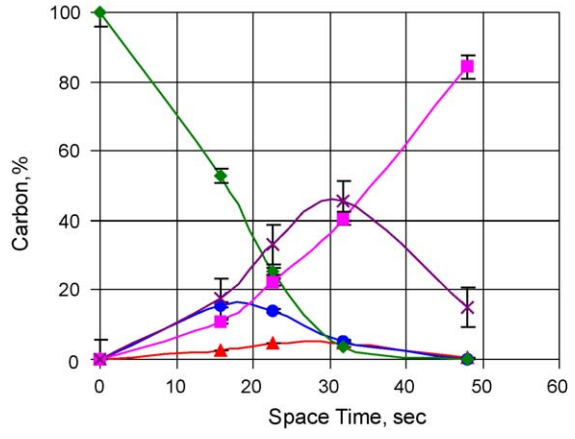

Fig. 7. Carbon balance of butyraldehyde over aerogel at the inlet butyraldehyde concentration of 243 ± 10 ppm molar and aerogel loading of 1.4 ± 0.05 mg/cm^2. Acetaldehyde (▲), propionaldehyde (●), butyraldehyde (◆), C in CO_2 (■), unmeasured chemicals (×).

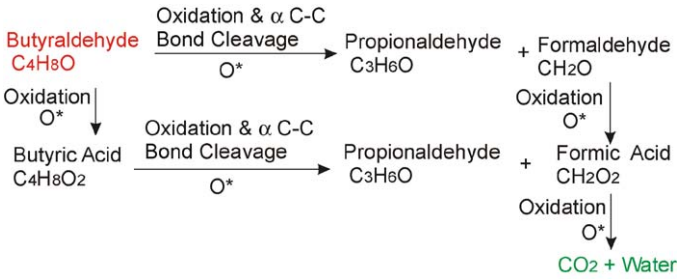

Fig. 8. Butyraldehyde PCO pathways via O^* mechanism.

Therefore, identified aldehydes and acids are the major byproducts of butyraldehyde PCO.

3.5. Further discussion of aldehyde PCO mechanism

Until now the deeper photocatalytic reaction mechanisms have not been well understood. In liquid phase, hydroxyl groups are widely accepted to initiate photocatalytic redox reactions [10,19], while in gas phase, adsorbed (and dissociated) oxygen (atom or ion) or lattice oxygen likely triggers the photocatalytic reactions [19–21]. As Herrmann proposed below, in gas phase PCO, a photoactive neutral, dissociated oxygen species O^* is the active species to initiate redox reactions [19].

$$(TiO_2) + h\nu \rightarrow e^- + h^+ \quad (1)$$

$$O_2(g) \leftrightarrow 2O(ads) \quad (2)$$

$$O(ads) + e^- \leftrightarrow O^-(ads) \quad (3)$$

$$O^-(ads) + h^+ \leftrightarrow O^*(ads) \quad (4)$$

With the humidity in the flow below 3 ppm molar, butyraldehyde PCO still took place at a healthy rate [15], which indicated that humidity was not necessary for aldehyde PCO in gas phase, due to abundant O_2 on the catalyst surface to initiate redox reactions. Extensive O_2 existence also suppressed the photo-Kolbe reaction [22] to propane, etc, so that no propane could be observed in butyraldehyde PCO. Butyraldehyde PCO pathways can be explained with oxygen species O^* as the key oxidant in a straightforward manner as shown in Fig. 8.

This mechanism suggests that the α-carbon in acids may go through formic acid before it is oxidized to CO_2. The α-carbon formic acid is difficult to observe. Muggli et al. [18] observed that CO_2 formed instantly during formic acid PCO, and no ^{13}C-byproducts could be detected during ^{13}C-acetic acid PCO. It is also possible that α-carbon in acids may directly oxidize to CO_2, but it should be less likely since it needs two active oxygen species at the same time.

$$CH_3CH_2CH_2COOH + 2O^*(ads) \rightarrow CH_3CH_2CHO + CO_2 + H_2O \quad (5)$$

If OH groups take part in reactions, the pathways should be:

$$CH_3CH_2CH_2CHO + 2HO^*(ads) \rightarrow CH_3CH_2CH_2OH + HCOOH \quad (6)$$

$$CH_3CH_2CHOH + HO^*(ads) \rightarrow CH_3CH_2CHO + H_2O \quad (7)$$

$$\text{or} \quad CH_3CH_2CH_2CHO + 2HO^*(ads) \rightarrow CH_3CH_2CH_2COOH + H_2O \quad (8)$$

$$CH_3CH_2CH_2COOH + 2HO^*(ads) \rightarrow CH_3CH_2CH_2OH + CO_2 + H_2O \quad (9)$$

Although Benoit-Marquie et al. reported significantly lower amount of propanol than propionaldehyde in gas phase butanol PCO [13], no propanol was detected in this study and other butanol PCO studies [11,12]. In gas phase PCO conditions the pathways involving hydroxyl groups were not favored compared to the active oxygen pathways. Propionaldehyde and acetaldehyde were oxidized in a similar fashion.

4. Conclusions

In this investigation, the reaction byproducts of aldehyde PCO were isolated from both the gas phase and the adsorbed phase. Liquid nitrogen was used to condense, trap and concentrate organic compounds from the reactor effluent, while deionized water was employed to extract the adsorbents on the TiO_2 photocatalyst. The compounds were identified with GC/FID and GC/MS after collection via a cryogenic device or an extraction step. The final products of aldehyde PCO were CO_2 and water, and the byproducts were corresponding acids and lower molecular-weight aldehydes/acids. The observed byproducts for butyraldehyde PCO were propionaldehyde, acetaldehyde, formaldehyde, butyric acid, propionic acid, acetic acid and formic acid. The carbon balance showed that acids, aldehydes, water, and CO_2, were major products of aldehyde PCO. Other byproducts, if any, were very low in quantity. The reaction pathways can be well explained with dissociated oxygen species O^* as well as OH group as the active oxidant. Other side reactions are suppressed, such as the hydroxyl oxidation to propanol and the photo-Kolbe reaction to propane, due to the presence of abundant oxygen.

Acknowledgments

Financial support from the Gulf Coast Hazardous Substance Center (Grant # 051LUB3744) and the Texas Higher Education Coordinating Board Advanced Technology Program (Grant # 003581-0019-1999) are gratefully acknowledged.

References

[1] A. Fujishima, K. Honda, Nature 238 (1972) 37–38.
[2] D.H. Chen, X. Ye, K. Li, Chem. Eng. Technol. 28 (2005) 95–97.
[3] L. Frazer, Environ. Health Perspect. 109 (2001) 4.
[4] M. Furuya, Annual Research Reports, Central Research Institute of Electric Power Industry, Japan, 2004.
[5] US EPA, Emergency Planning and Community Right-to-know Section 313, List of Toxic Chemicals, EPA260-B-01-001, March 2001.
[6] US Environmental Defense, Scorecard Pollution Information Site, 2006.
[7] US EPA, Pollution Prevention and Toxics, EPA 749-F-95-005a, December 1994.
[8] US EPA, Pollution Prevention and Toxics, EPA 749-F-94-003a, August 1994.
[9] C. Huang, D.H. Chen, K. Li, Chem. Eng. Commun. 190 (2003) 373.
[10] M. Smisek, S. Cerny, Active Carbon: Manufacture, Properties and Applications, Elsevier Publishing Company, New York, 1970.
[11] Y. Chapuis, D. Klvana, C. Guy, J. Kirchnerova, J. Air Waste Manage. Assoc. 52 (2002) 845.
[12] M.L. Sauer, D.F. Ollis, J. Catal. 158 (1996) 570–582.
[13] F. Benoit-Marquie, U. Wilkenhoner, V. Simon, A.M. Braun, E. Oliveros, M.T. Maurette, J. Photochem. Photobiol. A: Chem. 132 (2000) 225–232.
[14] J. Peral, D.F. Ollis, J. Catal. 136 (1992) 554–565.
[15] X. Ye, D. Chen, K. Li, V. Shah, M. Kesmez, K. Vajifdar, Chem. Eng. Commun., in press.
[16] X. Ye, Selected Topics on VOC Photocatalysis, Lamar University, 2003.
[17] N.R. Blake, G.L. Griffin, J. Phys. Chem. 92 (1988) 5697.
[18] D.S. Muggli, J.T. McCue, J.L. Falconer, J. Catal. 173 (1998) 470–483.
[19] J.M. Herrmann, Helv. Chim. Acta 84 (2001) 2731–2750.
[20] N. Djeghri, S.J. Teichner, J. Catal. 62 (1980) 99–106.
[21] D.S. Muggli, J.L. Falconer, J. Catal. 191 (2000) 318–325.
[22] B. Kraeutler, A.J. Bard, J. Am. Chem. Soc. 100 (1978) 5985–5992.